Excitations from dissociative fragments produced in $H^+ + H_2O$ collisions

Michael N. Monce, Sihui Pan,* Nadezhda L. Radeva, and Jaime L. Pepper†
Daghlian Accelerator Laboratory, Department of Physics, Astronomy, and Geophysics, Connecticut College, New London, Connecticut 06320, USA

(Received 27 August 2008; published 14 January 2009)

We report on photon emissions in the 200–800 nm region resulting from collisions of 200 keV protons with H_2O. The most prominent features observed in the spectrum are the Balmer series of hydrogen and two OH molecular bands. Several less intense O^+ as well as neutral O lines are also observed. The absolute photon emission cross sections of the major lines and bands were measured. The results indicate that a primary dissociation pathway involves the formation of H_2O^+ by removing a $1b_2$ electron. The unstable H_2O^+ ion further dissociates into $H^+ + OH$ or $OH^+ + H$. The dominant presence of neutral hydrogen lines and O^+ lines leads to the conclusion that the subsequent dissociation of OH^+ into $H + O^+$ prevails over the other possible dissociation pathway leading to H^+ and neutral oxygen fragments.

DOI: 10.1103/PhysRevA.79.012704 PACS number(s): 34.50.Fa, 34.50.Gb, 95.30.Dr, 96.25.Qr

I. INTRODUCTION

The water molecule certainly is one of the more ubiquitous found in the Earth's environment, in biological systems, and also in astrophysical environments. It should be of no surprise that much interest is devoted to interactions of various ions with this molecule.

Recently, there has been renewed interest in the spectroscopy of water [1], and also electron impact dissociation of H_2O [2]. Impact from protons and other ions in the energy ranges of 10 keV up to several MeV has received much attention in the last several years [3–6]. Much of the motivation for these studies appears to be in the radiolysis of water, but interests in astrophysical processes are also cited. These studies have focused on ionization of the target, and measurement of positive ion fragments following dissociation.

Despite the large interest in ion-water collisions, we report here what appears to be the first complete spectrum of photon emission from proton impact in the 200–800-nm-wavelength range. The first report of excitations from ion impact on water was a qualitative study of a mixed ion beam by Polykova *et al.* [7]. Nussbaum and Cathers reported on the 306-nm OH band produced by proton impact [8] and also other ions [9] in the 50–250-keV range. The last reported study is that of Yousif *et al.* [10] of Balmer-α emission for 3–100-keV proton impact which recorded both target and projectile emissions. Except for the study by Polykova *et al.*, the others report cross section measurements for the photon emission which were obtained by normalization to the well-studied 391.4-nm band of N_2^+ [11,12]. Pressure measurements were made with ionization gauges displaced from the target region, or even McLeod gauges. Spectrum and photon counting was done with a photomultiplier tube (PMT) where often the slit widths had to be adjusted so that a reasonable portion of a molecular band could be integrated. As such, the reported uncertainties in the cross sections are as high as 50%. With more modern measurement techniques employed in the current work our uncertainty for cross section is on average 8% [13], with the maximum of 12% due to peak fitting error.

II. EXPERIMENTAL DETAIL

Many of the details regarding the experimental techniques utilized in this laboratory can be found in previous publications [13,14]. These details include the accelerator system, beam measurement, target pressure measurement, as well as spectrometer wavelength calibration and efficiency measurement.

A major change in the experimental arrangement since our previous publications is in the target chamber and spectrometer. A new spectrometer-CCD (charge-coupled device) system was installed utilizing an Acton 0.5-m spectrometer fitted with two 1200-line/mm gratings blazed at 500 and 300 nm with a nominal resolution of 0.08 nm. The new CCD is a 1340×100 pixels liquid-nitrogen-cooled camera which greatly reduces the dark current. The new system is more efficient than our previous spectrometer-CCD unit by about a factor of 8.

Another major change is a new target chamber. While the interior design of the chamber with regard to the beam collimator, target gas cell and Faraday cup are virtually identical to the previous chamber, the major change is in the viewing angle of the spectrometer system. As shown in Fig. 1, we now view the collision region at the so-called "magic angle" of 56.47° [11]. At this angle the need to correct the measurements for polarization of the emitted radiation is eliminated. Also, we are now able to distinguish between projectile and target emission via Doppler shifted lines.

A stainless steel vacuum-secure vessel was constructed for the source of the water vapor. Approximately 10 ml of triply distilled water is placed in the vessel and a cold finger was immersed in liquid nitrogen in order to freeze the water. The temperature of the ice was monitored by a calibrated thermistor. It was found that if the ice was kept at a temperature of close to −4.0 °C, then a reasonable flow of water vapor through sublimation would be attained. The vessel was

*Present address: Department of Physics, Brandeis University, Boston, MA.
†Present address: Harvard College Observatory, Cambridge, MA.

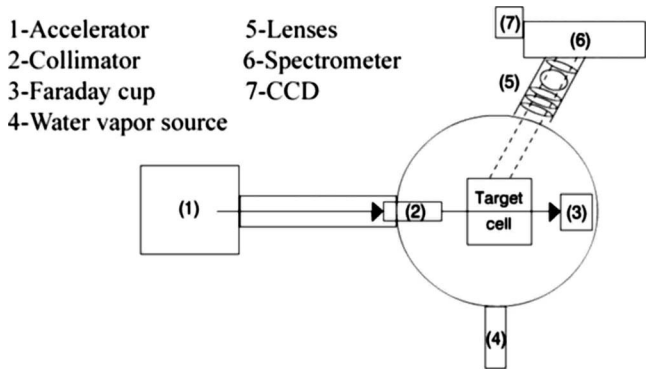

FIG. 1. Basic experimental system of accelerator, target chamber, and optical system.

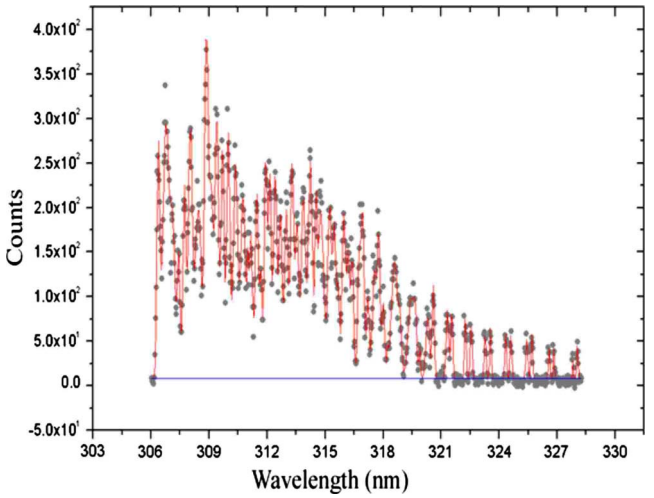

FIG. 2. (Color online) Illustration of the peak fitting used to determine total photon counts.

connected to the gas cell in the target chamber via a needle valve. The target gas pressure was kept close to a value of 3 mTorr. At this pressure, and with typical beam currents of 1 μA, we saw a linear variation in photon emission with beam current and target pressure so that single-collision conditions were assured. Initially, as we introduced water vapor to the target region we monitored the photon emission from the 391.4-nm band of N_2^+. We did not start the actual measurements on the proton-water collisions until the N_2^+ emission was reduced to near background thus insuring that outgassing of the water had been completed.

Spectra were obtained by simultaneously recording integrated beam current, target pressure, and temperature, while the CCD was exposed for times of 30–180 min. The optical efficiency of the system was calibrated using a standard lamp [11,13] and was generally flat from 800 nm down to 350 nm, then decreased rapidly down to 200 nm due to the CCD sensitivity. This is the primary reason for the differing integration times. Spectra were taken in 30-nm segments which allowed us to slightly overlap each spectrum for wavelength alignment purposes. All spectra were corrected for bias, flat field, and dark current. We then normalized each 30-nm segment for system efficiency based on the value of the efficiency of the system at 660 nm. We chose this value due to the fact that the efficiency is very flat at this wavelength. We also corrected each segment to a "standard" value of pressure, temperature, and total beam current so that differences in these values between data collection runs are taken into account.

As we have measured the efficiency of our optical system we are able to calculate absolute photon emission cross sections from our data. Following from Thomas [11,15] the cross section, without the need for polarization correction, is given by

$$\sigma = \frac{4\pi b\beta}{NI}\left[\frac{E}{S}\right]S_{ij}, \tag{1}$$

where b is the width of the standard lamp filament used in the efficiency calibration (0.12 cm), β is the spectral resolution of the system (0.08 nm), N is the target density in molecules/cm^3, and I is the projectile current in particles/sec. $[E/S]$ is the efficiency factor for the system at the particular wavelength under measurement and is derived from measuring the photon emission from the standard lamp divided by the known emission rate. This factor is given in units of emission/cm^2 of solid angle per nm bandwidth. Finally, S_{ij} is the measured photon count rate from the actual proton-target impact.

In order to measure the photon counts for a particular line or band, we import the spectral data into OriginPro [16] and then use the peak fitting routine in the software on each line to obtain a photon count. While atomic lines were easily fit with Gaussian curves, the most difficult part of this procedure was in fitting the molecular bands which involved individual fitting of the internal structure of the band. Figure 2 shows the 306-nm OH band and the fit obtained.

As a check that our procedure was producing reasonable values we measured the cross section for the previously mentioned 391.4-nm band of N_2^+. The most accurate value of this cross section appears to be that by Thomas [11] which is an un-normalized value of 1.05×10^{-17} cm^2 ($\pm25\%$). We measure a value of 8.9×10^{-18} cm^2 with the previously stated uncertainty of 12%. The two values overlap with respect to uncertainty. The absolute variation between the values would be attributable to the obvious differences in techniques from 1968 to the present work.

III. RESULTS AND DISCUSSION

The spectrum obtained by impacting H_2O with 200-keV protons is shown in Fig. 3. We chose the beam energy of 200 keV for two reasons: First, the accelerator provides a reasonably large output in beam current that is very stable at this energy. Second, previous experience in this laboratory and other studies have shown that the cross sections for photon emission generally peak towards the lower energies of 50–100 keV, and then fall off rapidly above 400 keV. As this was the first attempt at getting a spectrum from this collision process, 200 keV gives us a good compromise between beam stability or output and emission cross section. Lower energies provide less beam and stability, but larger

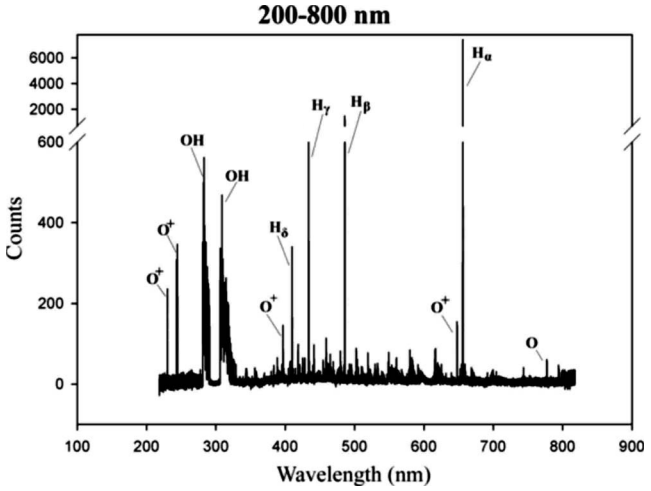

FIG. 3. Spectrum of $H^+ + H_2O$ collision at 200-keV beam energy. The spectrum has been corrected for instrument sensitivity and differences in target pressure, temperature, and total integrated beam.

cross sections. Higher energies provide more beam, but a quickly decreasing cross section.

As can be seen, the spectrum is dominated by the Balmer series of hydrogen, the well-known OH bands, and several O^+ lines. The Balmer lines are from target emission rather than from electron capture processes. We did detect, at a very low count, the Doppler shifted H_α line at the wavelength expected for the projectile velocity and viewing angle. It is too small to be seen in the spectrum as scaled.

Between 500 and 650 nm there appears to be a series of possible molecular bands of relatively low yield. We have not identified these bands. Also interspersed along the wavelength range are, other than the lines identified, faint O^+, as well as some neutral oxygen lines, such as the 777-nm O triplet labeled on the figure.

For the prominent lines shown, we measured the emission cross section as outlined in the previous section of the paper. The results are given in Table I. The uncertainty in the cross section values is 12%.

TABLE I. Photon emission cross sections for the major features seen in the collision spectrum produced in $H^+ + H_2O$ collisions at 200 keV. Uncertainty is 12%.

λ (nm)	Species	σ (cm^2)
648	O^+	2.4×10^{-20}
656	H_α	6.6×10^{-19}
486	H_β	1.3×10^{-19}
434	H_γ	5.2×10^{-20}
410	H_δ	2.7×10^{-20}
397	O^+	1.2×10^{-20}
306	OH band	8.9×10^{-19}
280	OH band	6.7×10^{-19}
230	O^+	1.7×10^{-20}
244	O^+	1.4×10^{-20}

Comparison of our H_α cross section to that as measured by Yousif *et al.* is difficult as their data terminate at a beam energy of 100 keV at which their cross section is 1.08×10^{-17} cm^2. Their data are normalized to previous work [17] which in turn is normalized to the N_2^+ of Thomas [12]. Thus while they state a net uncertainty of 20%, it may rise as high as 50%. Previous work from this laboratory [18] has shown that at these energies photon emissions cross sections generally fall off as $1/E$ with projectile energy. Using this model we estimate Yousif *et al.*'s cross section at 200 keV to be 5.4×10^{-18} cm^2 which is about a factor of 10 larger than our reported value. Other than differences in techniques, it is difficult to account for the discrepancy.

When we compare our 306-nm OH band result to that of Nussbaum and Cathers [8], the results are better. They report two cross sections at 150 and at 250 keV. Taking the average between these values yields $(1.75\pm0.9)\times10^{-18}$ cm^2 for 200 keV. This compares to our value of $(8.9\pm1.0)\times10^{-19}$ cm^2 and the values overlap within their respective uncertainties. However, Nussbaum and Cathers normalized their cross section to an earlier N_2^+ value that Thomas has shown to be in error [11]. By using the more accurate later value by Thomas [12] we can adjust their cross section to $(5.8\pm3.0)\times10^{-19}$ cm^2 which also overlaps our value within the uncertainties. The differences can perhaps be accounted for by our fitting of all the observed structure within the band, and also difference in target pressure measurements, use of digital imaging, etc.

Gobet *et al.* [4] have given a very good summary of the overall data with regard to ionization processes in the proton-water collision which shows a large decrease in the electron capture cross section above 100-keV beam energy. This is consistent with our observation of very little H_α emission from the projectile.

The valence electronic structure of water consists of the $(2a_1)^2(1b_2)^2(3a_1)^2(1b_1)^2$ orbitals in order of increasing energy [19]. Tan *et al.* [20] through a photoionization study have identified dissociation pathways for the H_2O^+ ion. The dissociation proceeds mainly through removal of $1b_2$ and $2a_1$ electrons. In particular they identify the $1b_2$ state as leading to both $H^+ + OH$ and also $OH^+ + H$ dissociations. Using Tan *et al.*'s results as also applied to their own study of positive ion production from proton-water collisions, Luna *et al.* [6] suggest that the excited OH^+ ion formed in the $1b_2$ dissociation channel can further lead to the following pathways:

$$(OH^+)^* \rightarrow H + O^+, \tag{2}$$

$$(OH^+)^* \rightarrow H^+ + O. \tag{3}$$

The presence of neutral OH, H, O, as well as O^+ emissions from our spectrum certainly indicate that all these processes are occurring. However, the dominance of the neutral hydrogen emissions, and also the relative preference of O^+ over neutral oxygen emissions, suggest that the process (2) above is a preferred channel once $OH^+ + H$ is formed from the removal of a $1b_2$ electron.

IV. CONCLUSIONS

We have presented the spectrum in the 200–800-nm wavelength range of photon emission produced in collisions of 200-keV H^+ with H_2O. The results show the presence of OH molecular bands and the Balmer series of hydrogen. We have measured absolute cross sections for these emissions. The results indicate that excited neutral fragments also arise in the dissociation of the water molecule. We suggest that our results indicate, when taken with other measurements of positive ion production, that a primary pathway involves a removal of a $1b_2$ electron to form H_2O^+ which then leads to dissociation of both $(OH)^*+H^+$, as well as $(OH^+)^*+H$. However, the presence of strong H emissions suggests that the subsequent dissociation of the $(OH^+)^*$ molecular ion favors fragmentation into neutral H^* and $(O^+)^*$.

We plan in the future to measure the emission cross sections for the prominent lines in the spectrum over the collision energy range of 50-400 keV. These data should give an indication of how the process of dissociation into neutral excited fragments changes with collision energy. For example we would expect to observe more Doppler shifted Balmer lines at the lower energies as the electron capture process increases in probability.

ACKNOWLEDGMENTS

This work was supported in part by a NASA-EPSCOR grant from the Connecticut Space Grant Consortium. Student support was provided by the Keck Undergraduate Science Program, Connecticut College. We also thank the referees for their helpful comments.

[1] Peter F. Bernath, Phys. Chem. Chem. Phys. **4**, 1501 (2002).
[2] S. W. J. Scully, V. Senthill, M. B. Shah, E. C. Montenegro, Phys. Rev. A **73**, 040701 (2006).
[3] F. Gobet, B. Farizon, M. Farizon, M. J. Gaillard, M. Carre, M. Lezius, P. Scheier, and T. D. Mark, Phys. Rev. Lett. **86**, 3751 (2001).
[4] F. Gobet *et al.*, Phys. Rev. A **70**, 062716 (2004).
[5] E. C. Montenegro and H. Luna, Braz. J. Phys. **35**, 927 (2005).
[6] H. Luna *et al.*, Phys. Rev. A **75**, 042711 (2007).
[7] G. N. Polyakova, Ya. M. Fogel, and Ch'iu Yu-mei, Sov. Astron. **7**, 267 (1976).
[8] Gilbert H. Nussbaum and Arthur R. Cathers, J. Chem. Phys. **65**, 4170 (1976).
[9] Gilbert H. Nussbaum and Arthur R. Cathers, J. Chem. Phys. **68**, 2521 (1978).
[10] F. B. Yousif, J. Geddes, and H. B. Gilbody, J. Phys. B **19**, 217 (1986).
[11] E. W. Thomas, *Excitations in Heavy Particle Collisions* (Wiley-Interscience, New York, 1972).
[12] E. W. Thomas, G. D. Bent, and J. L. Edwards, Phys. Rev. **165**, 32 (1968).
[13] Jennifer E. Kiehling *et al.*, J. Geophys. Res. **106**, 26147 (2001).
[14] Thomas F. Ammirati *et al.*, J. Geophys. Res. **110**, A04214 (2005).
[15] Desta Tadesse, Honors thesis, Connecticut College, New London, CT, 2005.
[16] OriginLab Corporation, Northhampton, MA.
[17] I. D. Williams, J. Geddes, and H. B. Gilbody, J. Phys. B **15**, 1377 (1983).
[18] Michael N. Monce, Phys. Rev. A **34**, 2780 (1986).
[19] John R. Van Wazer and Ilyas Absar, *Electron Densities in Molecules and Molecular Orbitals* (Academic, New York, 1975).
[20] K. H. Tan *et al.*, Chem. Phys. **29**, 299 (1978).